RSC Advances

ROYAL SOCIETY OF CHEMISTRY

www.rsc.org/advances

Journal Name

ARTICLE

Design and development of a nanoemulsion system containing extract of *Clinacanthus nutans* (L.) leaves for transdermal delivery system by D-optimal mixture design and evaluation of its physicochemical properties

Received 00th January 20xx,
Accepted 00th January 20xx

DOI: 10.1039/x0xx00000x

www.rsc.org/

Intan Soraya Che Sulaiman,*[a] Mahiran Basri,*[a] Hamid Reza Fard Masoumi,[a] Siti Efliza Ashari[a] and Maznah Ismail[b]

Clinacanthus nutans Lindau (*C. nutans*) is a well-known medicinal plant in South-East Asia that recently has attracted attention for its therapeutic characteristics and cosmeceutical applications. However, delivering the beneficial attributes of the bioactive ingredients into formulation is challenging due to poor solubility and low bioavailability of bioactive substances, which may hinder their effective transdermal delivery. Therefore, nanoemulsion has been chosen to be a carrier in encapsulation of bioactive ingredients *C. nutans* extract for pharmaceutical and cosmeceutical formulations. In this work, a D-optimal mixture design was used to determine the optimal composition of nanoemulsion-based system loaded with *C. nutans* leaves extract. The ultimate goal of the present work was to determine the optimum level of five independent variables (surfactant, oil, xanthan gum, bioactive extract, and water) in the optimal *C. nutans* nanoemulsion composition with minimum average droplet size. Under the optimal conditions, the predicted average droplet size was 99.99 nm. The actual response showed that the model was in good agreement with the predicted value with residual standard error (RSE) of 2.61%. The optimal nanoemulsion composition was observed to be stable under an accelerated stability study during storage at 25 and 45 ˚C for 90 days, centrifugal force and freeze–thaw cycles. Physicochemical characterizations of the optimal nanoemulsion showed its suitability for transdermal application due to its stability against phase separation.

Introduction

Belonging to the Acanthaceae family, *Clinacanthus nutans* Lindau is a shrub native to tropical Asian countries. *C. nutans* extracts are widely employed in Thai folk medicine as a remedy for insects bites.[1,2] Abundantly found in Malaysia, *C. nutans* is locally known as Sabah Snake Grass or Belalai Gajah. Among Malaysians, *C. nutans* is one of the most common herbs used in complementary and alternative medicine in cancer patients to slow down cancer progression and for symptom relief.[3] Singaporean communities consume *C. nutans* as traditional medicine for general detoxification purposes.[4] The medicinal use of this plant is scientifically supported by numerous reports on *C. nutans* properties such as anti-inflammatory,[5] anti-herpes simplex,[6,7] antioxidant and anti-cancer,[8] This medicinal plant, rich in phenols exhibits good antioxidant properties with better protection of plasmid DNA against riboflavin photoreaction in comparison to green tea.[9]

Consumers are increasingly environmentally conscious. Natural pharmaceutical and cosmetic products have gained tremendous attention compared to synthesized products for their fewer and less harmful side effects. Formulating a product with the beneficial attributes of the bioactive ingredients is a challenge due to various reasons such as poor solubility and low bioavailability of bioactive substances, which may hinder their effective transdermal delivery.[10–12]

In pharmaceutical and cosmeceutical formulations, encapsulation is currently under study for the production of an improved delivery system to gain an excellent end product. Emulsion is one of the delivery systems that use encapsulation. Oil-in-water (O/W) emulsion is a system that incorporates hydrophobic bioactive substances from a natural extract into the formulation. By definition, emulsion is a dispersion of one liquid phase in another immiscible liquid phase by using a mechanical device.[13] Nanoemulsion is an emulsion with a very fine droplet size in the diameter range of 20-200 nm. Due to their very fine droplet size, nanoemulsions possess excellent stability against sedimentation or creaming, which appears to be a challenging issue in emulsion stabilization.[14,15]

[a]*Nanodelivery Group, Department of Chemistry, Faculty of Science, Universiti Putra Malaysia, 43400 UPM Serdang, Selangor, Malaysia.*
E-Mail: IntanSulaimanUPM@yahoo.com (Intan Soraya Che Sulaiman); mahiran@upm.edu.my (Mahiran Basri)
[b]*Laboratory of Molecular Biomedicine, Institute of Bioscience, Universiti Putra Malaysia, 43400 Serdang, Selangor, Malaysia*

Changing the size of a particle from a macro to nano dimension can change its property. Due to the large surface area of the system, low surface tension and low interfacial tension, O/W nanoemulsions containing bioactive substances can effectively penetrate and be uniformly deposited at target sites.[10,15] In general for transdermal application of pharmaceutical and cosmeceutical products require the successful delivery of active ingredients through the skin's lipid barrier to reach the targeted lower layers. However the main resistance to transdermal transport is in a layer of cells joining the stratum corneum to the epidermis. Taking advantage of the nanosized molecule, the bioactive substances may pass through the pores and hair follicles of the skin and mucosal membranes, without disrupting normal tissues.[16,17] Moreover encapsulation technique may able to protect unstable and sensitive bioactive substances against unwanted degradation.[18] Furthermore, nanoemulsion are relatively non-toxic and safe and thus suitable for transdermal cosmetic application. Besides, nanoemulsions which are apparently transparent or translucent with low viscosity make them aesthetically pleasing, which is preferred in the pharmaceutical and cosmeceutical industries.[14]

D-optimal mixture design is a systematic design, oriented for formulation optimization which contains many ingredients. The design is not only the actual amount of each of the single ingredient, but also its proportion in relation to other ingredients. In a mixture design approach, the total sum of all ingredients is equal to 100%.[19] Each independent variable has effects on the experimental region and model making.[20] This multivariate statistical technique required less sample preparation than the traditional method, and therefore D-optimal mixture design is more preferable among researchers.[21,22] Nowadays, D-optimal mixture design has been adopted to optimize the cosmetic emulsions,[23,24] self-emulsifying drug delivery systems,[25] soap[26] and lipstick[27] formulation. Those studies demonstrated the advantages of D-optimal design in formulation and optimization of delivery systems. To date, application of *C. nutans* is limited in conventional formulation for treatment of herpes simplex and varicella zoster virus.[6,28] However, no study has been conducted on its potential in nanotechnology for pharmaceutical and cosmeceutical application. In addition, there are no published works on the optimization of *C. nutans* formulation using any multivariate statistical technique.

Therefore, the main objectives of this study were to produce and develop an optimal novel composition of *C. nutans* O/W nanoemulsion using D-optimal mixture design with minimum surfactant concentration and to identify the effect of the main components to the system. The physicochemical properties and stability of the optimal prepared nanoemulsion were determined.

Experimental

Materials and methods

Test materials. Fresh leaves of *C. nutans* were collected from a botanical farm in Jelebu, Negeri Sembilan, on January, 2014. The plant was authenticated by biologist Associate Prof. Dr. Rusea Go. The voucher specimen number (RG5125) was deposited at the Herbarium Unit of Universiti Putra Malaysia. All solvents and reagents were of analytical grade. Ethyl acetate, ethanol, n-hexane, dichloromethane, xanthan gum, polyoxyethylene sorbitan monooleate (T80), sorbitan monooleate (S80), 2-phenoxyethanol, guava seed oil (GSO) were obtained from Sigma-Aldrich (Germany). Palm kernel oil esters (PKOEs) were synthesized in our laboratory.[29] Deionized water was purified using the Milli-Q water system (EMD Millipore, Billerica, MA, USA).

Extract preparation. Fresh leaves of *C. nutans* were air-dried under sun shade and ground to fine powder. The fine powder was sequentially soaked in n-hexane, dichloromethane, ethyl acetate and ethanol. All extractions were collected separately. Ethanol and ethyl acetate were chosen for formulation due to their higher antioxidant activity demonstrated than our previous study.[8] Both extracts were filtered, and concentrated by using a rotary evaporator (Rotavapor R-210, Buchi, Switzerland) at approximately 40 °C and stored at -20 °C prior to further analysis.

Determination the solubility of *C. nutans* extract in oil mixture. To evaluate the potential of bioactive precipitation in the mixture of PKOEs:GSO, various ratios of oil mixture (PKOE:GSO) 9:1, 8:2 and 7:3 was added to the basic compositions. The composition of the 0.1% bioactive-loaded systems was added into the oil phase containing T80:S80, and 2-phenoxyethanol. The mixture was heated up to 70 °C until homogenized before subjected to centrifugal force for 15 min at 4000 rpm. Evaluation under cross-polarized light was made to observe possible phase separation. The best amount of oil mixture was observed as 9:1 in the composition formulation.

Formulation optimization

Experimental design. The experimental mixture design was employed to study the effect of five variable components of the *C. nutans* nanoemulsion: surfactant (A); oil (B); xanthan gum (C); bioactive extract (D); and water (E), on the response variable: the mean droplet size (Y). 2-phenoxyethanol was added into the formulations as an antimicrobial agent at 0.8% (w/w). The constraints of independent variables proportions are presented in Table 1.

Table 1 Constraints of independent variable proportions

Independent variables, *Xj*	Lower limit, *Lj*	Upper limit, *Uj*
Surfactant, A	7	13
Oil, B	5	15
Xanthan gum, C	0.5	1
Bioactive extract, D	0.05	0.1
Water, E	70.1	86.65

By using Design Expert software (Version 7, Stat. Ease Inc., Minneapolis, USA), the design matrix was generated. According to the D-optimal mixture design, the input variables

are non-negative proportionate amounts of mixture, therefore the sum must be equal to one, as shown below,

$$\sum X_j = 1 \qquad and\ 0 \leq X_j \leq 1$$

Formation of nanoemulsion containing *C. nutans* extract. Formulations containing *C. nutans* extract were prepared by a combination of high (high shear homogenizer) and low energy (overhead stirrer) emulsification methods. The oil used was a mixture of PKOEs and GSO in a ratio of 9:1. GSO was chosen to blend with PKOEs as its providing a good source of linoleic acid. Linoleic acid is an essential fatty acid that can enhance the absorption of bioactive extract and also can be used as carrier oil.[30–32] The bioactive material was a mixture of ethyl acetate and ethanol extracts of *C. nutans* leaves (1:1). The blend of hydrophilic (Tween 80) and lipophilic (Span 80) non-ionic surfactants at ratios 8.2:1.8 were chosen to obtain better solubilization and stability of the dispersion system developed. Initially, the aqueous and oil phase mixtures were prepared separately and heated up to 70 °C. Once each mixtures were homogenized, the oil phase consisting of T80:S80, PKOEs:GSO, bioactive, and 0.8% (w/w) 2-phenoxyethanol was gradually added drop wise to the aqueous phase (xanthan gum and deionized water) and stirred with Ultra Turax high shear homogenizer (T25 digital, IKA-Werk, Germany) for 15 min at 6000 rpm. The emulsions were then cooled down to room temperature (25 ± 0.5 °C) by mixing, using an overhead stirrer (RW20 digital, IKA-Werk, Germany) at 250 rpm speed for 30 min.

Statistical analysis

Analysis of variance (ANOVA) was performed to determine the significant differences between the independent variables. Reduced model ($p < 0.05$) and multiple regressions were employed in analyzing the experimental data.

Verification of the model

In order to access the adequacy of the final reduced model, a few random formulations were prepared to validate the model prediction. The percentage of the residual standard error (RSE) was calculated for each response.

Characterization of the optimal composition of nanoemulsion containing *C. nutans* extract

Mean particle size, zeta potential and polydispersity index (PDI) measurement. The particle size, long term stability and size distribution of molecules in nanoemulsions system were measured by dynamic light scattering (DLS) droplet size analyzer (Zetasizer Nano ZS90, Malvern Instruments, UK. The samples were diluted (1:200) with deionized water before being filled into a cuvette capillary cell to avoid multiple scattering effects. Measurements were performed with an angle of 173° at room temperature (25 ± 0.5 °C).

Transmission electron microscopy (TEM). The size and morphology of optimal nanoemulsion were analyzed by using transmission electron microscopy (Hitachi H7100, Japan). Samples were diluted in deionized water and homogenized. A Formvar coated copper grid was placed on top of a drop of diluted sample and left at room temperature (25 ± 0.5 °C) for 3 min. The samples on the filled copper grid were stained using 2% phosphotungstic acid for 2 min and air-dried prior to analysis.

Rheological measurement. The viscosity of optimal nanoemulsion was measured by Kinexus Rotational Rheometer (Malvern Instruments, UK). The measurement was performed at a temperature of 25.0 ± 0.5 °C with 4°/40 mm cone and plate geometry and gap of 0.100 mm. The steady rheological behavior of the emulsion was measured at a controlled rate varying from 0.1 to 100 s^{-1}. The sample was allowed to stand for 10 min after being loaded in order to reach equilibration prior to measurement.

Thermogravimetric analysis (TGA). The thermal property of the nanoemulsion was studied by TGA/SDTA851 (Metler Toledo, Switzerland). Liquid nitrogen was used as a gas carrier in the system. Temperature ranged from 50 to 600 °C. The sample was loaded into the instrument in the aluminum pan and the empty pan was set as a reference.

Accelerated stability study. The stability study for optimal nanoemulsion involved the following: stability under storage for three months at room temperature (25 ± 0.5 °C) and 45 °C; stability under centrifugation, and freeze thaw cycles. In the centrifugation test, the sample was subjected to centrifugal force for 15 min at 4000 rpm. Optimal nanoemulsion was also tested in a freeze thaw cycle by placing the sample in a vial and freezing the sample at -4 °C for 12 h. The sample was then thawed at room temperature for another 12 h. This step was repeated 3 times. Evaluation under cross-polarized light was made to observe possible phase separation.

pH determination. The pH measurement of the optimal nanoemulsion was performed at room temperature (25 ± 0.5 °C) by using a Delta 320 pH meter (Mettler-Toledo, Switzerland). The pH measurement is important to assess whether the sample is compatible with human skin.

Conductivity measurement. The conductivity of the optimal nanoemulsion was measured using a Conductometer S230 Seven Compact (Mettler-Toledo, Switzerland). Conductivity value determines the amount of free ions in the system.

Fourier transforms infrared spectroscopy (FT-IR). The chemical stability of *C. nutans* extract in developed nanoemulsions system was studied by recording the FT-IR spectra of the freshly prepared nanoemulsions (2 days) compared to nanoemulsions storage in 25 °C and 45 °C after one year. The samples were analysed by attenuated total reflection (ATR) technique using Perkin Elmer Spectrum 100 FT-IR Spectrometer in the range of 4000-280 cm^{-1}.

Results and discussion

Solubility of *C. nutans* extract in oil

The solubility of *C. nutans* extract in oil mixture at various ratios was determined. Under centrifugal force, all mixture did not show any precipitation at the bottom of the test tube. It

showed that PKOEs oil makes a good combination with GSO oil in oil phase. PKOEs were selected as based oil in the formulation to blend with GSO due to its properties as good carriers for active ingredients in formulation. Compare with other carrier oil used in pharmaceuticals and cosmetics, PKOEs is cheaper than jojoba oil.[33] Moreover PKOEs which consists of shorter chain esters provided better storage and thermal stability characteristics, nontoxic, less greasy and excellent wetting behaviour.[29] Nutritional values of PKOEs oil can be enhance to produce modified oil enriched with polyunsaturated fatty acid. By blend it with other edible oil such as GSO which consists of 74.6% of linoleic acid can provide better oils by enhanced it bioactive absorption property.[30,32] The solubility of *C. nutans* extract in all mixture showed no precipitation. As the cost of PKOEs is much cheaper, ratio of 9:1 (PKOE: GSO) was chosen as the best amount of oil mixture to be used in the formulation.

Model fitting

Experimental and predicted data analysis for the effect of five variables of nanoemulsion containing *C. nutans* extract on the particle size is shown in Table 2. Using the Design Expert software, a quadratic model was the best fit of all the models (linear, special cubic, cubic). 2-Phenoxyethanol was added into the formulations at constraints 0.8% (w/w). The predicted values obtained by model fitting compared well with the observed values.

Table 2 Experimental data, actual and predicted values obtained from the D-optimal model

Experiment No.	A	B	C	D	E	Particle size (nm)	
						Actual	Predicted
1	7.031	5.005	0.672	0.100	86.392	137.7	138.65
2	9.773	8.408	0.990	0.099	79.930	164.84	163.86
3	12.998	9.857	0.650	0.100	75.595	126.33	124.54
4	12.979	12.554	0.780	0.092	72.794	176.9	179.17
5	12.998	15.000	0.501	0.055	70.646	228.9	229.42
6	7.756	15.000	1.000	0.050	75.394	604.2	603.58
7	7.225	14.744	1.000	0.100	76.131	827.3	824.14
8	13.000	5.084	0.753	0.072	80.290	40.12	41.69
9	7.031	5.005	0.672	0.100	86.392	139	138.65
10	7.000	8.495	0.500	0.071	83.134	232.03	231.62
11	7.225	14.744	1.000	0.100	76.131	820.1	824.14
12	12.997	15.000	0.999	0.089	70.116	237.3	237.88
13	9.644	14.998	0.670	0.100	73.788	376.9	375.56
14	9.402	5.001	0.500	0.050	84.246	87.63	84.90
15	7.756	15.000	1.000	0.050	75.394	604.33	603.58
16	13.000	10.150	1.000	0.055	74.996	143.05	140.98
17	9.708	11.843	0.716	0.050	76.883	237.85	241.68
18	12.998	15.000	0.501	0.055	70.646	230.6	229.42
19	9.402	5.001	0.500	0.050	84.246	83.26	84.90

In order to examine the suitability and significance of the final model, an analysis of variance (ANOVA) was employed using Design Expert software (Table 3).

The computed F-value of the model (9225.19) indicated that the model design was significant. This result showed that predicted and actual values revealed good correspondence between them, and the model developed can be used to adequately describe the relationship between the variables to the response and to predict the particle size of optimal *C. nutans* nanoemulsion. Regression coefficient for the final reduced model is presented in Table 4.

Table 3 ANOVA results for the effect of the five variables

Source	Sum of Squares	DF	Mean square	*F*-Value	*p*-Value	Significance
Model	1059782.80	11	96343.89	9225.19	< 0.0001	significant

Linear Mixture	920620.95	4	230155.24	22037.98	< 0.0001	
AB	7205.60	1	7205.60	689.96	< 0.0001	
AC	21339.10	1	21339.10	2043.28	< 0.0001	
AD	1629.37	1	1629.37	156.02	< 0.0001	
AE	2912.40	1	2912.40	278.87	< 0.0001	
BD	1150.64	1	1150.64	110.18	< 0.0001	
BE	572.98	1	572.98	54.86	0.0001	
CE	917.77	1	917.77	87.88	< 0.0001	
Residual	73.11	7	10.44			
Lack of Fit	35.34	2	17.67	2.34	0.1918	not significant
Pure Error	37.77	5	7.55			
Cor Total	1059855.90	18				

The final equation for the model obtained was shown in equation (1). The greatest effect on the response was caused by factor C (xanthan gum). This could be due to the presence of hydrocolloid gum such as xanthan gum can affect the non-Newtonian behavior of emulsions.[34] This phenomenon was a consequence of a decrease in the non-Newtonian behavior of emulsion during which an overlap of xanthan gum concentration in the aqueous phase was reached.[34,35] As stabilizer added to the emulsion, xanthan gum acts by modifying the viscosity of the aqueous phase.[36] By increasing the viscosity of the continuous phase, the emulsion stability was enhanced and thus retarded the droplets movement.[37] As the result, the particle size of the molecules decreased with increasing amount of xanthan gum. Some studies reported that addition of xanthan gum to the emulsion may minimize droplet mobility and decreases collision numbers. Hence, it provided enough time for surfactant to adsorb on droplets and stabilize them from coalescence.[35,38] However, at certain concentration of xanthan gum, the depletion flocculation occurs. After this overlapping concentration, increasing amount of xanthan gum will promote creaming through mechanism of depletion.[35] Therefore the particle size of molecules after this concentration started to increase. Figure 1 represents that the polynomial regression model was in good agreement with the experimental results. The predicted R^2 of 0.9989 was in reasonable agreement with the adjusted R^2 of 0.9998. The signal to noise ratio of 304.663 indicated an adequate signal; thus the model can be used to navigate the design space in order to predict the particle size of *C. nutans* nanoemulsion.

Table 4 Regression coefficient results for the final reduced model

Source	Coefficient estimate	Regression coefficient	Particle size
A-Surfactant	2018.91	Standard deviation	3.23
B-Oil	386.85	PRESS	1161.79
C-Xanthan gum	17139.05	R^2	0.9999
D-Bioactive extract	-2366.40	Adjusted R^2	0.9998
E-Water	108.89	Predicted R^2	0.9989
AB	-3265.49	Adequate precision	304.663
AC	-48123.31		
AD	-165054		
AE	-2423.56		
BD	101121.90		
BE	241.33		
CE	-13410.46		

Journal Name

ARTICLE

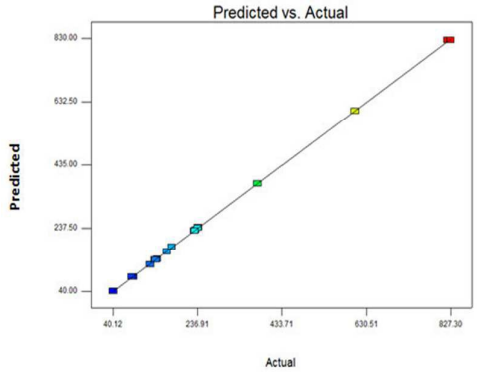

Fig. 1 Comparison of predicted and actual values of particle size of nanoemulsion.

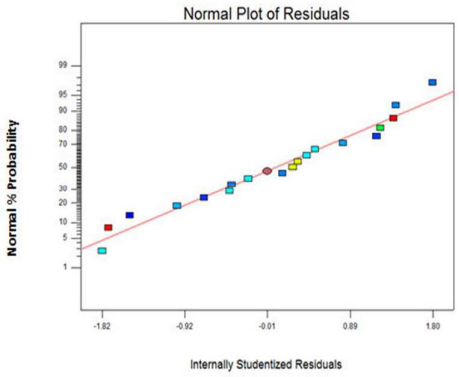

Fig. 2 Normal plot of the residuals.

The model obtained is shown in regression equation (1).

$$Y = 83778.50A - 6323.40B + 564763.61C + 214014.35D - 54.23E - 119220.74AB - 1756950.25AC - 6026012.61AD - 88482.76AE + 3691892.72BD + 8810.94BE - 489606.91CE \quad (1)$$

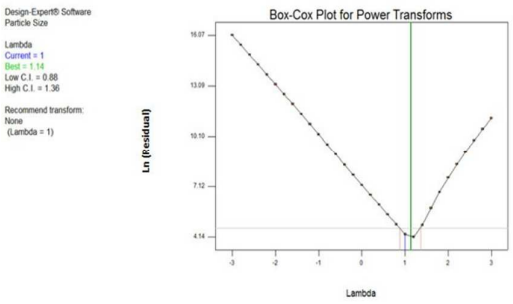

Fig. 3 Box-Cox Plot.

D-Optimal analysis

By using D-Optimal analysis, a diagnostic test is performed on the normal distribution of the residual and any transformations are confirmed in the Box-Cox plot (Figures 2 and 3). Lambda values refer to the power raised by the transformation. The ideal lambda value is at the lowest point of the Box-Cox plot. The predicted and ideal values were 1 and 1.14 respectively, which is close to the actual value. Therefore none transformation is required.

In order to assess the effect of each variable on the particle size of *C. nutans* nanoemulsion, the three-dimensional (3D) surface and contour (2D) plots were examined. The plots presented in Figure 4 demonstrate the influence of surfactant, oil, and xanthan gum on the response. The other two independent parameters (bioactive extract and water) were kept constant. Decreasing the surfactant concentration increased the particle size of the nanoemulsion. This might have been due to a low level of emulsifier concentration that led to the incomplete surface coverage of oil; hence, oil droplets coalesced and led to an increase in particle size.[39] Surfactants can reduce interfacial tension, therefore with insufficient amounts of surfactant oil was less homogenized in the aqueous phase, which increased particle size.[40]

In contrast, decreasing the oil concentration seemed to decrease of the particle size of emulsion from 524.23 nm to 126.69 nm. This could be due to a lower collision rate between oil droplets, which reduces the possibility of coalescence.[41] Sufficient emulsification results in smaller particle sizes.[42] Xanthan gum, however behaves differently. By increasing xanthan gum concentration, particle sizes decreased but at a certain level, particle size starts to increase. The same observation was reported by Krstonošić et al. (2015) and Rodd et al. (2000) in the presence of xanthan gum as an emulsifier.[34,43] As mentioned earlier, decrease in non-Newtonian behavior of emulsion happened because xanthan gum reached overlap concentration in which individual polymer molecules begin to physically interact. Therefore, after that concentration, the flocculation occurs and the droplets form a weak-gel network. Thus, promoted a large particle size to be produced.[34,43]

Journal Name

ARTICLE

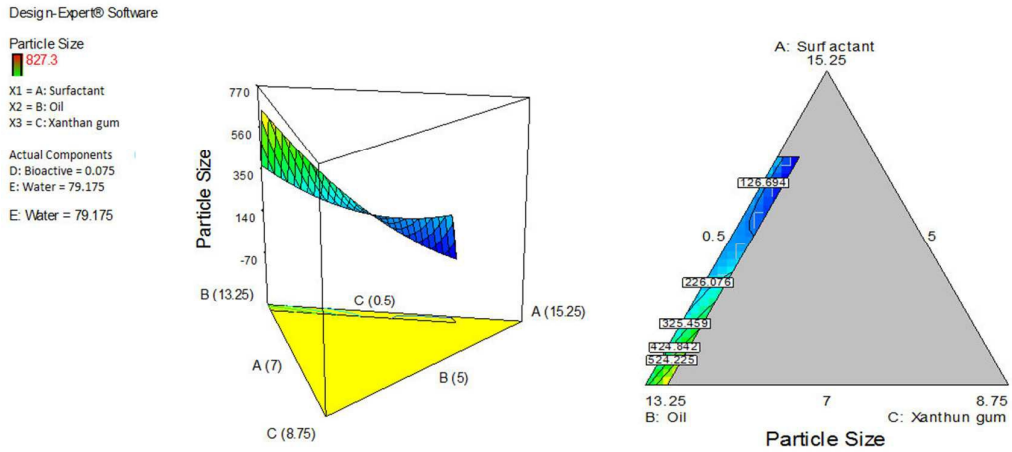

Fig. 4 The 3D surface and 2D plots illustrated the effect of three variables: surfactant (A), oil (B) and xanthan gum (C) on the particle size of nanoemulsion; bioactive extract (D) and water (E) are kept constant.

The 3D surface and 2D plots presented in Figure 5 demonstrate the influence of the bioactive extract on the response. Direct interactions can be observed in the presence of the bioactive extract. Increasing the amount of the bioactive extract results in a significant increased of particle size from 275.84 nm to 439.32 nm. Therefore, the incorporation of bioactive extract into the particles will result incremental increased of particle size.[44]

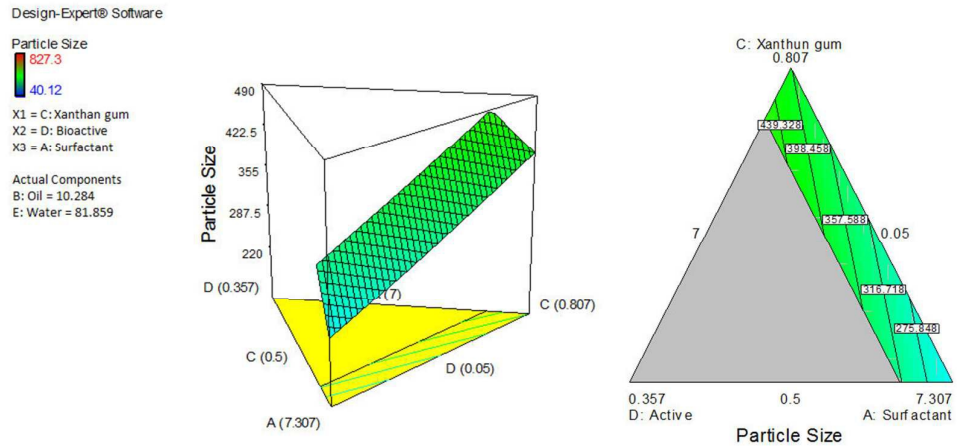

Fig. 5 The 3D surface and 2D plot demonstrate the influence of bioactive extract (D) on the particle size of nanoemulsion; and oil (B) and water (E) are kept constant.

Verification of the model

In order to determine the adequacy of the final model, seven randomized formulations were performed to verify the model (Table 5). Results were compared to predicted values by calculating the residual standard error (RSE %);

$$\text{Residual standard error } (\%) = \frac{Actual\ value - Predicted\ value}{Predicted\ value} \times 100 \qquad (2)$$

The RSE% indicated no significant difference between the actual and predicted values, proving that a good model was obtained.

Table 5 Predicted and actual response values for randomized formulations

Variables					Particle size (nm)		RSE (%)
Surfactant (%)	Oil (%)	Xanthan gum (%)	Bioactive (%)	Water (%)	Actual	Predicted	
9	7.5	1	0.075	82.745	145.17	145.348	0.12
10.2	9.5	0.73	0.075	79.495	173.20	172.974	0.13
10.4	10	0.74	0.075	78.785	177.50	182.236	2.60
10.7	10.5	0.76	0.075	77.965	187.80	188.474	0.36
11	11	0.77	0.075	77.155	191.70	193.626	0.99
11.2	11.5	0.8	0.075	76.425	199.60	202.78	1.57
11.5	12	0.85	0.075	75.575	210.03	209.34	0.33

Optimization of responses

An optimum formulation of *C. nutans* nanoemulsion was determined to contain optimum levels of five independent variables (surfactant, oil, xanthan gum, bioactive extract, and water) with minimum particle size. Bioactive agents can be more effective if the particle size is small to obtain successful delivery of active ingredients through the skin barrier.[45] Due to a large surface area, nano-sized systems can offer rapid penetration and deposit uniformly on substrates.[15] However, smaller particle sizes may be obtained with higher surfactant levels but the optimum formulation would have the surfactant at a minimum. High level of surfactant will exposed the skin to irritation as well as increases the cost of production.

Table 6 The constraints used in numerical optimization

Name	Goal	Lower limit	Upper limit	Importance
Constraints				
Surfactant	Minimize	7	13	3
Oil	In range	5	15	3
Xanthan gum	In range	0.5	1	3
Bioactive	Maximize	0.05	0.1	5
Water	In range	70.92	87.19	3
Particle size	In range	90	100	5

Taking into account the constraints of Table 6, the optimum formulation of *C. nutans* nanoemulsion was obtained with a composition of 5% of oil, 8.13% of surfactant, 1% of xanthan gum, 0.1% of bioactive extract, 0.8% of preservative and 84.97% of water. Under the optimum compositions, the predicted average droplet size is 99.99 nm, whereas the actual size was 97.38 nm. The actual response showed that the model is in good agreement with the predicted value with a residual standard error (RSE) of 2.61%.

Characterization of developed nanoemulsion containing *C. nutans* extract

Under the optimum composition, mean particle size, zeta potential and polydispersity index (PDI) were 97.38±1.63 nm, -25.1±0.57 mV and 0.25±0.01, respectively (mean ± standard deviation). Zeta potential value measured electrokinetic potential of a particle. The formulation with having zeta potential value higher than +25 mV and lower than -25mV indicate that the formulation system is stable. This is due to the ability of the particle surface charge to prolong the stability

of the formulation by electrostatic repulsion.[46] The zeta potential values of *C. nutans* nanoemulsion prepared indicated the formulation has long term stability. Polydispersity index measured the size distribution of molecules or particles in the formulation. It described how much light is scattered from the various sizes. The PDI value of the optimal formulation in range of 0.1–0.25 indicated a narrow size distribution.[47]

TEM images (Figure 6) confirmed the spherical shape of oil droplets in a colloidal system and encapsulation of the bioactive extract in the oil droplets. Apart from that, the particle size measured using TEM is in accordance with the size procured from photon correlation spectroscopy.

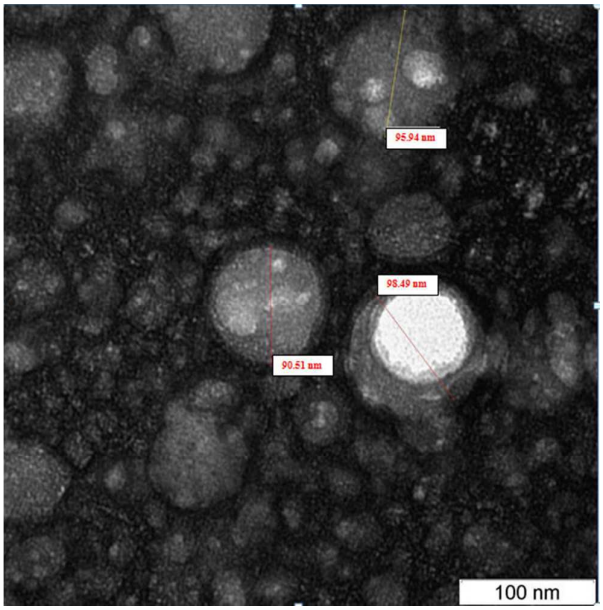

Fig. 6 TEM images of encapsulated nanoemulsion with bioactive extract.

Two rheological experiments (steady state and oscillatory) were employed for a better understanding of the behavior of respective nanoemulsion. The *C. nutans* nanoemulsion had a shear-thinning behavior in both experiments. Figure 7 represents result of the steady state experiment; shear stress versus shear rate. This direct interaction indicated the present of pseudoplastic behavior in the system,[48] which fitted with the Power Law Model shown in following equation (3);

$$\tau = k\gamma^n \qquad (3)$$

Whereas τ is the shear stress (Pa), γ is the shear rate (s^{-1}), *k* is the fluid consistency index ($Pa.s^n$) and *n* is the flow behavior index (dimensionless). Pseudoplastic behavior is one of the important criteria in formulation of transdermal applied cosmetic and pharmaceutical products. Therefore the property of pseudoplastic formulation has low resistance to flow when applied under high shear condition and zero flow under gravity stress.[24] According to oscillatory result presented in Figure 8, the dominant value of G' over G" (storage and loss modulus, respectively) defines the gel structure existence.[49] This appearance of the structure is due to the droplet network association from the depleting flocculation.[50]

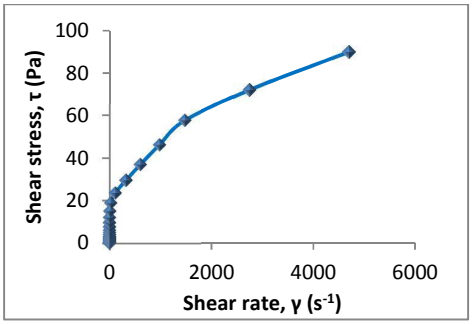

Fig. 7 Flow curve of shear stress (Pa) *versus* shear rate (s^{-1}).

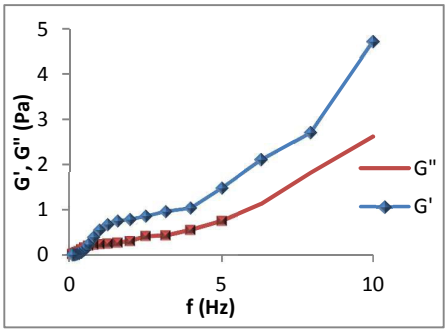

Fig. 8 Plot of G' and G" *versus* frequency.

Thermogravimetric analysis (TGA) has been employed to study the degradation temperature of nanoemulsion. The TGA thermogram (Figure 9) demonstrated three distinct transformation regions, with a mass loss observed in the system. The first change occurred at the range of 60 °C to 185 °C due to the loss of water from the surface. This is followed by the second change at the temperature range of 225 to 350 °C due to the loss of water in the micelle structure. At very high temperatures, approximately 350 to 440 °C, decomposition of oil occurs, due to the combustion of organic-bound carbon in the oil. With rapid heating, the transformations over higher temperatures occur in shorter times but over broader temperature ranges.[51]

The nanoemulsion prepared under optimum compositions was defined to be stable upon centrifugal force test and freeze thaw cycles (Table 7). With different storage conditions for 90 days (room temperature and 45 °C), no phase separations were observed, indicated the stability of the nanoemulsion.

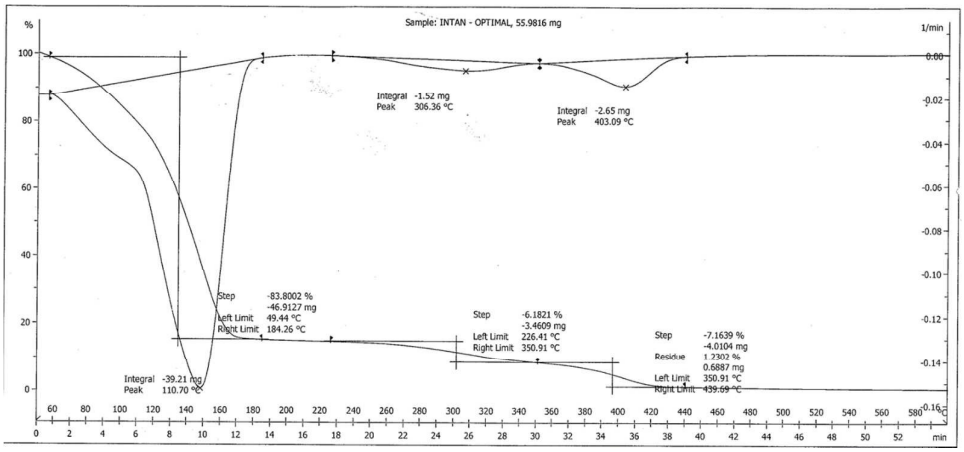

Fig. 9 TGA thermogram of nanoemulsion.

Table 7 Storage stability

Stability test	Storage stability (Days) 1		30		60		90		Centrifugation	Freeze thaw cycle (3 cycles)
Temperature (°C)	25	45	25	45	25	45	25	45		
	√	√	√	√	√	√	√	√	√	√

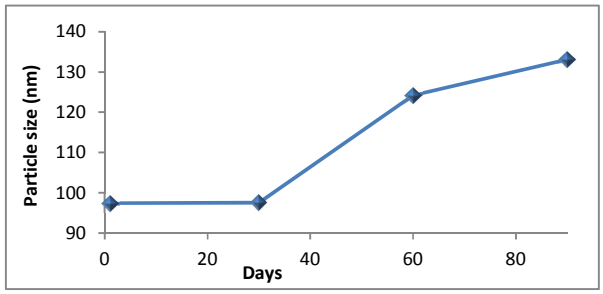

Fig. 10 Particle size observed (90 days) for stable optimal nanoemulsion at 25 °C.

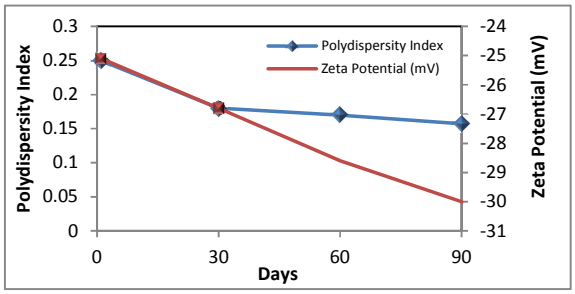

Fig. 11 Polydispersity index and zeta potential for stable optimal nanoemulsion at 25 °C.

The stability of the end product under extreme storage conditions is important to ensure the ability of the final formulation to tolerate under market storage. For better understanding of the stability assessment for optimal formulation at room temperature (25 °C), the particle size, polydispersity index and zeta potential changes during observation period for 90 days was recorded (Fig. 10 and Fig. 11). Even though, the particle sizes of the colloidal system slightly increased in time during the storage period however still remaining in the nano-sized range (less than 200 nm). This phenomenon could be attributed to Ostwald ripening and coalescence. Coalescence can be preventing by a stabilizer while Ostward ripening will continuously occur. Ostward ripening is defined as the process in which large particles grow at the expense of the smaller particles due to the higher solubility of smaller ones.[52] The pH value for optimal nanoemulsion was 5.27±0.01. This pH value is compatible with the pH of human skin which ranges from 5 to 6.[53] Conductivity tests can be used to determine the ability of the emulsion to conduct electricity. High conductivity values will lead to less lamellar water and more free water in the system.[54] Moreover, high conductivity indicates that the aqueous phase is the continuous phase in the system. Thus, the type of nanoemulsion can be determined as either oil in water (O/W)

or water in oil (W/O). In this study, C. nutans nanoemulsion was confirmed as an O/W nanoemulsion due to its high conductivity value of 1227 µS/cm. Furthermore, oil in water formulation was more favourable in formulation of cosmetic product due to its characteristic such as less greasy and less cost. Fig. 12 illustrates the FT-IR spectra of *C. nutans* nanoemulsions in different storage conditions. The spectra clearly show that the freshly prepared nanoemulsion (2 days) and the nanoemulsions for one year storage at 25 °C and 45 °C have no significant difference. This indicated the stability of *C. nutans* extract in developed nanoemulsions system showing no decomposition of the compounds against long term storage (one year) at different temperatures (25 °C and 45 °C).

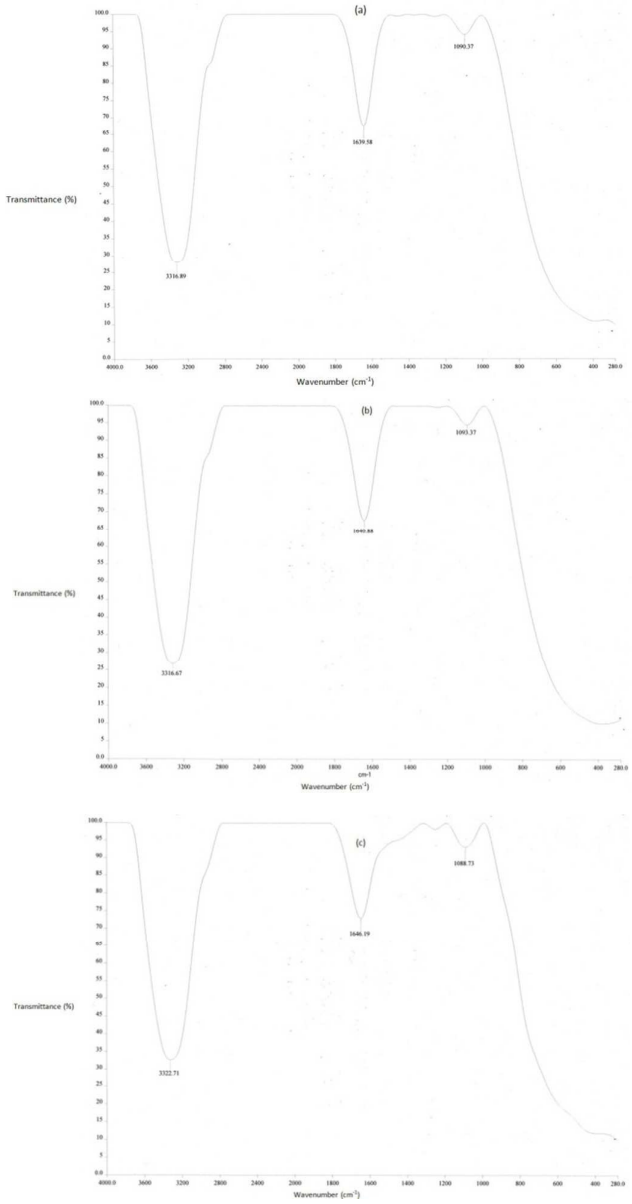

Fig. 12 FT-IR spectra of *C. nutans* nanoemulsions. (a) Freshly prepared (2 days), (b) One year storage at 25 °C and (c) One year storage at 45 °C.

Conclusions

By using D-Optimal mixture design, a quadratic polynomial model was successfully predicted and fitted to predict the optimal composition of *C. nutans* nanoemulsion. The model was verified statistically with ANOVA and diagnosed with D-optimal analysis. Experimental results were in good agreement with predicted values as residual standard error (RSE) for the optimal composition was 2.61%; therefore the model can be used to navigate the design space in order to predict the particle size of *C. nutans* nanoemulsion. All variables used in this study affected the parameter response (particle size) of the *C. nutans* nanoemulsion. The optimal composition of *C. nutans* nanoemulsion was revealed to be 5% oil, 8.13% surfactant, 1% xanthan gum, 0.1% bioactive extract, 0.8% preservative and 84.97% water. Characterization of the physicochemical properties of the optimal *C. nutans* nanoemulsion reveals it to be promising as a system for delivery of nature-based pharmaceutical and cosmetic products due to it long term stability.

Acknowledgement

The author would like to acknowledge financial support from Universiti Putra Malaysia (Vote. No GP-IPS/2014/9438735) and MyBrain 15 Postgraduate Scholarship Programme.

References

1 S. Sakdarat, A. Shuyprom, T. Na Ayudhya, P. Waterman and G. Karagianis, *Thai J. Phytopharm.*, 2006, **13**, 13–24.
2 X. P'ng, G. Akowuah and J. Chin, *Int. J. Pharm. Sci. Res.*, 2012, **3**, 4202–4204.
3 M. Farooqui, M. A. Hassali, A. K. A. Shatar, M. A. Farooqui, F. Saleem, N. U. Haq and C. N. Othman, *J. Tradit. Complement. Med.*, 2015, 8–13.
4 Y. Siew, S. Zareisedehizadeh, W. G. Seetoh, S. Y. Neo, C. H. Tan and H. L. Koh, *J. Ethnopharmacol.*, 2014, **155**, 1450–1466.
5 P. Wanikiat, A. Panthong, P. Sujayanon, C. Yoosook, A. G. Rossi and V. Reutrakul, *J. Ethnopharmacol.*, 2008, **116**, 234–244.
6 P. Kunsorn, N. Ruangrungsi, V. Lilipun, A. Khanboon and K. Rungsihirunrat, *Asian Pac. J. Trop. Biomed.*, 2013, **3**, 284–290.
7 C. Yoosook, Y. Panpisutchai, S. Chaichana, T. Santisuk and V. Reutrakul, *J. Ethnopharmacol.*, 1999, **67**, 179–187.
8 I. S. C. Sulaiman, M. Basri, K. W. Chan, S. E. Ashari, R. F. Masoumi and M. Ismail, *African J. Pharm. Pharmacol.*, 2015, **9**, 861–874.
9 J. M. P. Yuann, J. S. Wang, H. L. Jian, C. C. Lin and J. Y. Liang, *MC-Transaction Biotechnol.*, 2012, **4**, 45–58.
10 Y. Li, J. Zheng, H. Xiao and D. J. McClements, *Food Hydrocoll.*, 2012, **27**, 517–528.
11 J. Bevernage, J. Brouwers, S. Clarysse, M. Vertzoni, J. Tack, P. Annaert and P. Augustijns, *J. Pharm. Sci.*, 2010, **99**, 4525–4534.
12 A. González-Paredes, B. Clarés-Naveros, M. A. Ruiz-Martínez, J. J. Durbán-Fornieles, A. Ramos-Cormenzana and M. Monteoliva-Sánchez, *Int. J. Pharm.*, 2011, **421**, 321–331.
13 T. G. Mason, J. N. Wilking, K. Meleson, C. B. Chang and S. M. Graves, *J. Phys. Condens. Matter*, 2006, **18**, R635–R666.
14 C. Solans, P. Izquierdo, J. Nolla, N. Azemar and M. Garciacelma, *Curr. Opin. Colloid Interface Sci.*, 2005, **10**, 102–110.
15 T. Tadros, P. Izquierdo, J. Esquena and C. Solans, *Adv. Colloid Interface Sci.*, 2004, **108-109**, 303–318.
16 C. Sinico and A. M. Fadda, *Expert Opin. Drug Deliv.*, 2009, **6**, 813–825.

17 A. Ammala, *Int. J. Cosmet. Sci.*, 2013, **35**, 113–124.
18 V. Devarajan and V. Ravichandran, *Int. J. Compr. Pharm.*, 2011, **02**, 1–6.
19 H. R. Fard Masoumi, M. Basri, W. Sarah Samiun, Z. Izadiyan and C. J. Lim, *Int. J. Nanomedicine*, 2015, **10**, 6469–6476.
20 T. Lundstedt, E. Seifert, L. Abramo, B. Thelin, Å. Nyström, J. Pettersen and R. Bergman, *Chemom. Intell. Lab. Syst.*, 1998, **42**, 3–40.
21 Z. Jeirani, B. Mohamed Jan, B. Si Ali, I. Mohd. Noor, S. Chun Hwa and W. Saphanuchart, *Chemom. Intell. Lab. Syst.*, 2012, **112**, 1–7.
22 M. Bakhtiyari, M. Moosavi-Nasab and H. Askari, *Food Hydrocoll.*, 2015, **45**, 18–29.
23 J. Djuris, D. Vasiljevic, S. Jokic and S. Ibric, *Int. J. Cosmet. Sci.*, 2014, **36**, 79–87.
24 S. Samson, M. Basri, H. R. Fard Masoumi, R. Abedi Karjiban and E. Abdul Malek, *RSC Adv.*, 2016, **6**, 17845–17856.
25 E. B. Basalious, N. Shawky and S. M. Badr-Eldin, *Int. J. Pharm.*, 2010, **391**, 203–11.
26 F. P. Borhan, S. S. Abd Gani and R. Shamsuddin, *ScientificWorldJournal.*, 2014, **2014**, 1–8.
27 N. Kamairudin, S. S. A. Gani, H. R. F. Masoumi and P. Hashim, *Molecules*, 2014, **19**, 16672–16683.
28 S. Charuwichitratana, N. Wongrattanapasson, P. Timpatanapong and M. Bunjob, *Int. J. Dermatol.*, 1996, **35**, 665–666.
29 P. S. Keng, M. Basri, M. R. S. Zakaria, M. B. A. Rahman, a. B. Ariff, R. N. Z. A. Rahman and a. B. Salleh, *Ind. Crops Prod.*, 2009, **29**, 37–44.
30 C. Prottey, P. Hartop and M. Press, *J. Invest. Dermatol.*, 1975, **64**, 228–234.
31 A. Simopoulos, *Am. J. Clin. Nutr.*, 1991, **54**, 438–463.
32 N. Prasad and G. Azeemoddin, *J. Am. Oil Chem.*, 1994, **71**, 457–458.
33 E. Mahdi, A. Noor, M. Sakeena, G. Abdullah, M. Abdulkarim and M. Sattar, *Int. J. …*, 2011, **6**, 2499–2512.
34 V. Krstonošić, L. Dokić, I. Nikolić and M. Milanović, *Food Hydrocoll.*, 2015, **45**, 9–17.
35 V. Krstonošić, L. Dokić, P. Dokić and T. Dapčević, *Food Hydrocoll.*, 2009, **23**, 2212–2218.
36 E. Dickinson, *Food Hydrocoll.*, 2003, **17**, 25–39.
37 a Paraskevopoulou, *Food Chem.*, 2005, **90**, 627–634.
38 E. Makri and G. Doxastakis, *J. Sci. Food Agric.*, 2006, **86**, 1863–1870.
39 L. L. Hecht, C. Wagner, K. Landfester and H. P. Schuchmann, *Langmuir*, 2011, **27**, 2279–2285.
40 M. D. Triplett and J. F. Rathman, *J. Nanoparticle Res.*, 2008, **11**, 601–614.
41 S. Y. Tang, S. Manickam, T. K. Wei and B. Nashiru, *Ultrason. Sonochem.*, 2012, **19**, 330–345.
42 S. H. Musa, M. Basri, H. R. F. Masoumi, R. A. Karjiban, E. A. Malek, H. Basri and A. F. Shamsuddin, *Colloids Surf. B. Biointerfaces*, 2013, **112**, 113–119.
43 A. B. Rodd, D. E. Dunstan and D. V. Boger, *Carbohydr. Polym.*, 2000, **42**, 159–174.
44 Y. Liu and M. Nair, *J. Nat. Prod.*, 2010, **73**, 1193–1195.
45 B. Teo, M. Basri, M. Zakaria, A. Salleh, R. Rahman and M. Rahman, *J. Nanobiotechnology*, 2010, **8**, 4.
46 T. N. Barradas, V. E. B. de Campos, J. P. Senna, C. D. S. C. Coutinho, B. S. Tebaldi, K. G. D. H. E. Silva and C. R. E. Mansur, *Colloids Surfaces A Physicochem. Eng. Asp.*, 2014, **480**, 214–221.
47 V. Patravale and R. Kulkarni, *J. Pharm. …*, 2004, **56**, 827–840.
48 O. H. Campanella, N. M. Dorward and H. Singh, *J. Food Eng.*, 1995, **25**, 427–440.
49 N. G. Diftis, C. G. Biliaderis and V. D. Kiosseoglou, *Food Hydrocoll.*, 2005, **19**, 1025–1031.
50 I. . Mandala, T. . Savvas and a. . Kostaropoulos, *J. Food Eng.*, 2004, **64**, 335–342.
51 R. Speyer, *Thermal analysis of materials*, Marcel Dekker, Inc., 1993.
52 I. Capek, *Adv. Colloid Interface Sci.*, 2004, **107**, 125–155.
53 N. Akhtar, M. Ahmad, Gulfishan, I. Masood and M. Aleem, *Pak. J. Pharm. Sci.*, 2008, **21**, 430–437.
54 M. Korhonen, H. Niskanen, J. Kiesvaara and J. Yliruusi, *Int. J. Pharm.*, 2000, **197**, 143–151.